

Cavity-enhanced laser cooling of solid-state materials in a standing-wave cavity

Yuhua Jia (贾佑华), Biao Zhong (钟 标), and Jianping Yin (印建平)

State Key Laboratory of Precision Spectroscopy, East China Normal University, Shanghai 200062

Received January 21, 2008

We propose a new method to cool the Yb^{3+} -doped ZBLANP glass in a standing-wave cavity. There are two advantages of this cavity-enhanced technique: the pumping power is greatly enhanced and the absorption of the cooling material is greatly increased. We introduce the basic principle of the cavity-enhanced laser cooling and discuss the cooling effect of a solid-state material in a cavity. From the theoretical study, it is found that the laser cooling effect is strongly dependent on the reflectivity of the cavity mirrors, the length of the solid material, the surface scattering of the material, and so on. Some optimal parameters for efficient laser cooling are obtained.

OCIS codes: 160.2540, 300.2530, 140.3320.

doi: 10.3788/COL20080611.0848.

At the beginning of this century, Pringsheim suggested the possibility of cooling an object by using anti-Stokes fluorescence. In 1995, the first experimental evidence of laser cooling in a solid was presented, in particular, for an Yb^{3+} -doped fluorozirconate glass^[1]. From then on, several works have been published regarding topics such as the composition requirements of the matrices to achieve cooling and the temperature drop attainable in fiber configuration^[2–5]. Anti-Stokes fluorescence cooling solids may lead to the development of an all-solid-state cryogenic refrigerator that can be used for a variety of applications^[6,7]. Though a lot of progress has been made in laser cooling of solid-state materials, improvements toward some real applications of this laser cooling technology are still need. This is due to two main obstacles. One is the power of pumping laser needs to be several watts, and the pumping laser that meets this condition is rather expensive. The other is the whole cooling system is too big and too weighty for the loaded ability of cooling. In this letter, therefore, we propose a cavity-enhanced cooling scheme to overcome the first obstacle mentioned above and amend the current laser cooling results. We calculate the cooling process and theoretically analyze this cavity-enhanced cooling effect.

The cavity arrangement is shown in Fig. 1. Two Mirrors M_1 and M_2 compose a Fabry-Perot (F-P) cavity and their amplitude reflectivities are r_1 and r_2 respectively. We place a cooling material (Yb^{3+} -doped ZBLANP glass) inside this standing-wave F-P cavity, and then the pumping laser power in the cavity can be enhanced by 10 – 100 times compared with the incident laser power. If the length of the sample is L and the absorption coefficient is α , then according to the Beer's law,

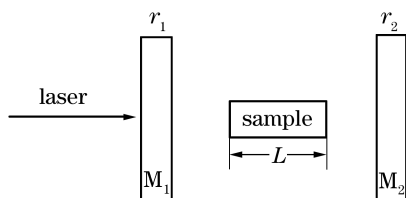


Fig. 1. Standing-wave cavity arrangement.

the absorption loss is $e^{-\alpha L}$ after a single pass through the material. At the same time, we must consider the intensity losses resulting from the reflection of the two ends of the sample. For the case of perpendicular incidence, the reflectivity of one optical surface can be described as

$$R_s = \left(\frac{n_0 - n_1}{n_0 + n_1} \right)^2, \quad (1)$$

where n_0 and n_1 are the refractive indices of the incident medium and the transmission one, respectively. Here we suppose $n_0 = 1$, $n_1 = 1.5$, so the intensity loss is about 4% when the incident light passes through one end-surface of the sample once. However, if we use a coating to increase its transmission, R_s can be reduced to 1%. It is quite important for the cavity-enhanced experiment. In this case, the circling intensity at last in the cavity is given by

$$I_{\text{cicr}} = \frac{2I_0}{1 + [r_1 r_2 (1 - R_s)^2 e^{-\alpha L}]^2 - 2r_1 r_2 (1 - R_s)^2 e^{-\alpha L}}, \quad (2)$$

where I_0 is the laser intensity after the first mirror and can be represented by the intensity of the initial input laser I as $I_0 = I(1 - r_1^2)$. And then we can obtain the cavity enhancement factor:

$$E_{\text{cav}} = \frac{I_{\text{cicr}}}{I} = \frac{2(1 - r_1^2)}{1 + [r_1 r_2 (1 - R_s)^2 e^{-\alpha L}]^2 - 2r_1 r_2 (1 - R_s)^2 e^{-\alpha L}}. \quad (3)$$

The absorption coefficient can be defined as the absorption cross section σ multiplied by the rare-earth doped ion's concentration N :

$$\begin{aligned} \alpha &= \sigma N = 3.7 \times 10^{-22} \text{ (cm}^2\text{)} \times 2.42 \times 10^{20} \text{ (cm}^{-3}\text{)} \\ &= 0.09 \text{ (cm}^{-1}\text{)}. \end{aligned} \quad (4)$$

Supposing $L = 3$ mm and $r_2 \approx 1$, we study the dependence of the cavity enhancement factor E_{cav} on the

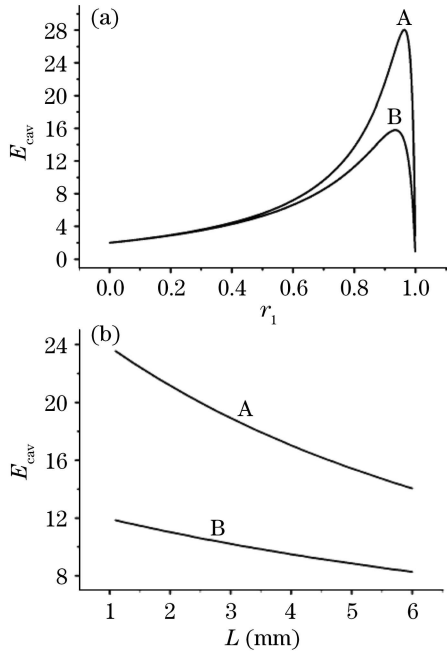


Fig. 2. (a) Relationship between the cavity enhancement factor E_{cav} and the reflectivity of the first mirror r_1 ; (b) relationship between the cavity enhancement factor E_{cav} and the sample length L . Curves A and B show the results with and without the coating, respectively.

reflectivity of the first mirror r_1 , and the results are shown in Fig. 2. Curve A in Fig. 2(a) describes the coating case of the cooling material ends with a reflectivity of $R_s = 0.01$, and curve B shows the calculation results without coating (i.e., $R_s = 0.04$). It is clear from Fig. 2(a) that when the reflectivity of the end-surface of cooling material is reduced from 0.04 to 0.01, the maximum cavity enhancement factor will be increased from about 15 to 28, and the corresponding optimal reflectivities of the first mirror are about 0.94 and 0.96, respectively.

We also study the relationship between the cavity enhancement factor E_{cav} and the length of the sample L , and find that E_{cav} is strongly dependent on L due to the absorption loss, especially in the case of coating the end surfaces of the sample, as shown in Fig. 2(b). When L is reduced from 6 to 1 mm, E_{cav} will increase from about 14 to 23. This shows that the dependence of the cavity enhancement factor on the length of the sample is very important in the laser cooling experiment.

From the above analysis, we know that the cavity-enhanced technique may greatly improve the cooling effect because of the cavity enhancement and the increasing of the absorbed power. Here we use a two-energy-level system to analyze the cooling power and discuss how the cavity enhancement influences the cooling result. First of all, the cooling power can be expressed as^[3]

$$P_{cool} = \frac{N\sigma_{abs}L\alpha_{eff}I_s(\lambda/\lambda_{F^*} - 1)}{1 + \sigma_{se}/\sigma_{abs} + \alpha_{eff}I_s/P}, \quad (5)$$

where α_{eff} is the effective pump-spot area, I_s is the characteristic wavelength-dependent saturation intensity, σ_{abs} and σ_{se} are the absorption and stimulated-emission cross sections, respectively, λ is the pumping wavelength,

P is the pumping power, λ_{F^*} is the effective mean emission wavelength.

Taking some parameters which are used in Mungan's experiment^[3] as input data, we study the dependence of the temperature drop on the pumping laser power and the results are shown in Fig. 3. We find that the cooling temperature will be reduced with the increase of the pumping power. For example, when the pumping power is increased from 0.22 W to 2.2 W, the cooling temperature will be reduced from about 294.6 to 280.5 K.

For high pumping power, the cooling effect is not greatly enhanced mainly due to the saturated absorption. According to the enhancement factor obtained above, we only need to use a pumping laser with a lower power of 100 mW even a few tens of milliwatts for efficient laser cooling, which can be satisfied by using a laser diode (LD) with a moderate power (10 – 100 mW).

Moreover, the cooling power can also be defined as^[8]

$$P_{cool} = P_{abs}\eta = P_{abs}\frac{\lambda - \lambda_f}{\lambda}, \quad (6)$$

where η is the quantum efficiency. If we suppose that η is a constant (actually η will be slightly reduced during the cooling process)^[9], the cooling power will be proportional to the absorbed power P_{abs} . In a cavity, we have

$$P_{abs} = P_{circ}[1 - \exp(-\alpha L)], \quad (7)$$

where P_{circ} is the circling power in the cavity. If we use coating technique to increase the transmission of the solid sample ends, from Eq. (7) we know that the absorbed power can be increased by 27 times. Even without coating, the absorbed power can also be increased by about 14 times.

In order to find the advantage of this cavity-enhanced cooling scheme, we compare it with the most popular multi-pass scheme used in solid cooling^[10], as illustrated in Fig. 4. In this configuration, the sample is placed

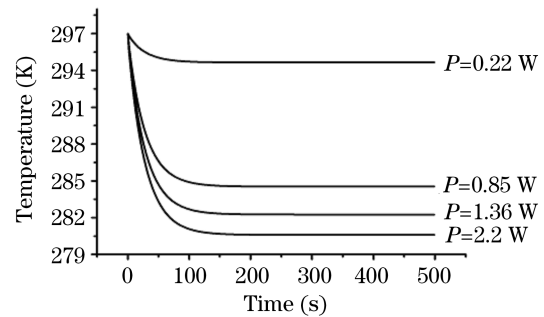


Fig. 3. Temperature drop under different pumping powers.

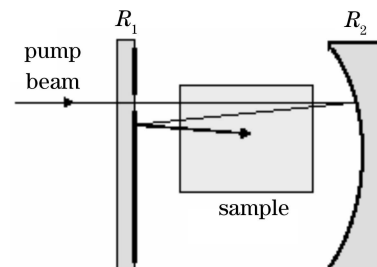


Fig. 4. Cavity arrangement for the multi-pass scheme.

on glass supports between two dielectric mirrors of high reflectance for the pumping beam. The beam passes through a small hole in the dielectric coating of a planar mirror. After the first pass through the sample, the pumping beam is reflected by a second mirror with a certain radius of curvature and back into the sample. The mirrors have been optimized so that the beam slightly misses the hole in the first mirror, resulting in multiple passes.

The total absorbed power in the multi-pass scheme is given by

$$\begin{aligned}
 P_{\text{abs}} &= P_{\text{in}} T_s [1 - \exp(-\alpha L)] \\
 &\times [1 + R_2 T_s^2 \exp(-\alpha L) + R_2 R_1 T_s^4 \exp(-2\alpha L) \\
 &+ R_2^2 R_1 T_s^6 \exp(-3\alpha L) + R_2^2 R_1^2 T_s^8 \exp(-4\alpha L) + \dots] \\
 &= P_{\text{in}} T_s [1 - \exp(-\alpha L)] \left[\frac{2 - 2(R_2 R_1 T_s^4 \exp(-2\alpha L))^n}{1 - R_2 R_1 T_s^4 \exp(-2\alpha L)} \right],
 \end{aligned} \tag{8}$$

where R_1 and R_2 are the reflectivities of the two mirrors, P_{in} is the input laser power, T_s represents the transmittance for one surface of the sample. To obtain the maximum value, we assume that the reflection times approach an infinite value, then Eq. (8) will turn into

$$P_{\text{abs}} = P_{\text{in}} T_s [1 - \exp(-\alpha L)] \left[\frac{2}{1 - R_2 R_1 T_s^4 \exp(-2\alpha L)} \right]. \tag{9}$$

Supposing $R_1 = R_2 = 99.9\%$ and $T_s = 96\%$, Eq. (9) can be reduced as

$$P_{\text{abs}} = 9.8 P_{\text{in}} [1 - \exp(-\alpha L)]. \tag{10}$$

From our calculation, we find that the cavity-enhanced cooling scheme can exceed the limit of the multi-pass scheme and result in a higher cooling power. So we think that the cavity-enhanced scheme is more efficient than the multi-pass scheme.

The relationship between the cooling power and the temperature can be expressed by^[11]

$$C_m \rho_m S \frac{d(T_{\text{sample}} - T_0)}{dt} = P_{\text{load}}(T_{\text{sample}}) - P_{\text{cool}}(T_{\text{sample}}), \tag{11}$$

where S is the cross section area of the sample, P_{load} is radiative and conductive heat load, C_m and ρ_m are the specific heat and the mass density, T_{sample} and T_0 represent the sample temperature and the room temperature, respectively.

Figure 5 illustrates the cooling results of the multi-pass scheme and the cavity-enhanced scheme. It is obvious that the cavity-enhanced cooling scheme is more efficient. In order to show it more clearly, we compare the cooling temperature of the sample in the case with or without coating. Figure 6 shows the dependence of the cooling temperature on the reflectivity of the surface of the solid sample ends. When the reflectivity of the

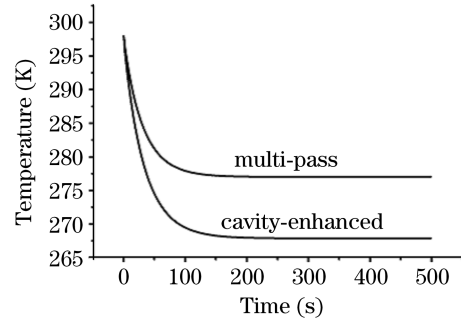


Fig. 5. Temperature comparison between the multi-pass scheme and the cavity-enhanced scheme.

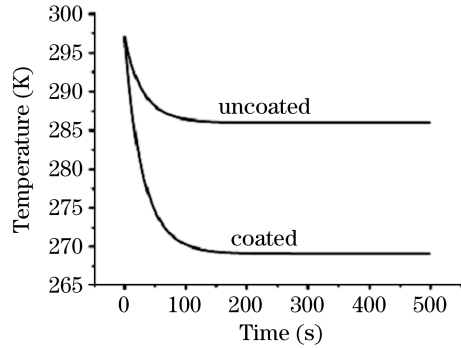


Fig. 6. Temperature comparison when the end surfaces of the sample are coated and uncoated.

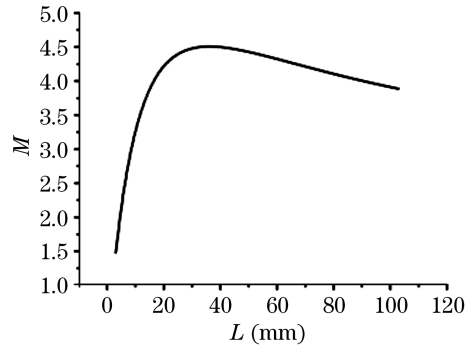


Fig. 7. Relationship between the improvement factor of cooling power M and the sample length L .

sample ends is reduced from 0.04 to 0.01, the temperature is decreased from about 286 to 268 K.

We have discussed two main reasons that influence the cooling effect, but the choice of the sample's length is still a crucial question. We know that a solid material with a longer length can improve the absorbed power, but it will increase the loss of the pumping intensity in the cavity. Therefore, there exists an optimal sample length in the cooling process^[12]. Figure 7 shows the dependence of the improvement factor of the cooling power on the sample length and calculation shows that the optimal length is about 3.6 cm. This result is very close to Rayner's experimental result^[2], for which a 4-cm-long fiber was used.

In conclusion, we have proposed a novel cavity-enhanced scheme to cool a solid sample and introduced the basic principle of the cavity-enhanced laser cooling. Taking the Yb^{3+} -doped ZBLANP glass as an example, we have also studied the dependence of the cooling temperature on the pumping power and discussed the

influences of the coating and the length of the sample on the laser cooling effect. The study shows that the laser cooling effect is strongly dependent on several parameters such as the reflectivity of the cavity mirrors and the length of the solid sample. In particular, the smaller the pumping laser power is, the larger the improvement factor of the cooling power will be; the lower the reflectivity of the sample ends is, the lower the cooling temperature will be. The optimal sample length is 3.6 cm. These results are beneficial to realize the laser cooling of the solid-state materials in the cavity by using a LD with a moderate power, which is experimentalized at present. As we know, diode lasers are relatively cheap and reliable sources of coherent radiation^[13–15]. It will be conducive to the popularization of the laser cooling experiment and its technical applications, even to the development of all-optical solid refrigerator.

This work was supported by the National Natural Science Foundation of China (No. 10434060 and 10674047), the Doctor Foundation of the Educational Ministry of Education of China (No. 20040269010), the Shanghai Priority Academic Discipline, the 211 Foundation of the Ministry of Education of China, and the PhD Program Scholarship Fund of East China Normal University (ECNU) 2007. J. Yin is the author to whom the correspondence should be addressed, his e-mail address is jpyin@phy.ecnu.edu.cn.

References

1. R. I. Epstein, M. I. Buchwald, B. C. Edwards, T. R. Gosnell, and C. E. Mungan, *Nature* **377**, 500 (1995).

2. A. Rayner, M. E. J. Friese, A. G. Truscott, N. R. Heckenberg, and H. Rubinsztein-Dunlop, *J. Mod. Opt.* **48**, 103 (2001).
3. C. E. Mungan, M. I. Buchwald, B. C. Edwards, R. I. Epstein, and T. R. Gosnell, *Phys. Rev. Lett.* **78**, 1030 (1997).
4. X. Luo, M. D. Eisaman, and T. R. Gosnell, *Opt. Lett.* **23**, 639 (1998).
5. A. Rayner, M. Hirsch, N. R. Heckenberg, and H. Rubinsztein-Dunlop, *Appl. Opt.* **40**, 5423 (2001).
6. B. C. Edwards, J. E. Anderson, R. I. Epstein, G. L. Mills, and A. J. Mord, *J. Appl. Phys.* **86**, 6489 (1999).
7. R. I. Epstein, J. J. Brown, B. C. Edwards, and A. Gibbs, *J. Appl. Phys.* **90**, 4815 (2001).
8. C. W. Hoyt, M. Sheik-Bahae, R. I. Epstein, B. C. Edwards, and J. E. Anderson, *Phys. Rev. Lett.* **85**, 3600 (2000).
9. G. Lamouche, P. Lavallard, R. Suris, and R. Grousseau, *J. Appl. Phys.* **84**, 509 (1998).
10. C. W. Hoyt, M. P. Hasselbeck, M. Sheik-Bahae, R. I. Epstein, S. Greenfield, J. Thiede, J. Distel, and J. Valencia, *J. Opt. Soc. Am. B* **20**, 1066 (2003).
11. T. R. Gosnell, *Opt. Lett.* **24**, 1041 (1999).
12. B. Heeg, G. Rumbles, A. Khizhnyak, and P. A. DeBarber, *J. Appl. Phys.* **91**, 3356 (2002).
13. J. Zhang, K. Huang, and D. Yang, *Chin. Opt. Lett.* **4**, 525 (2006).
14. J. Chen, J. Liu, Y. Zhang, W. Liu, R. Kan, M. Wang, D. Chen, and Y. Cui, *Acta Opt. Sin.* (in Chinese) **27**, 350 (2007).
15. S. Li, C. Li, and C. Song, *Acta Opt. Sin.* (in Chinese) **27**, 928 (2007).